Article

Effects of Heavy Rainfall on Shallow Foundations in Bukit Timah Granite in Singapore

Verasak Sia [1], Alfrendo Satyanaga [2] and Yongmin Kim [1,*]

1   School of Engineering, University of Glasgow, Singapore 138683, Singapore
2   Department of Civil and Environmental Engineering, Nazarbayev University, Nur-Sultan 010000, Kazakhstan
*   Correspondence: yongmin.kim@glasgow.ac.uk

Abstract: The increase in rainfall intensities due to climate change affect the entire globe. In particular, Singapore suffers from floods and rising of coastlines. Notably, in the Bukit Timah Region in Singapore, floods are getting more intense, and the region houses multitudes of low-rise constructions with shallow foundations. Damages ranging from physical, in terms of motor vehicle and property damages, to intangible losses such as major traffic delays in both private and public transit were caused by the floods. Few studies have been carried out in Singapore in terms of shallow foundations' response to rainfall events. When rainfall infiltrates into the soil, the bearing capacity and soil stiffness are affected by the change in matric suction. Thus, the impact of heavy rainfall on shallow foundations in Bukit Timah Granite is investigated numerically using SIGMA/W. Fully coupled flow-deformation analysis with unsaturated soil characteristics, e.g., the Soil Water Characteristic Curve (SWCC) and unsaturated permeability functions, were conducted. A range of rainfall intensities, rainfall durations, and applied loadings were investigated to produce a load–settlement curve that was compared against a semi-empirical model to yield reasonable results. The studies showed that the change in matric suction is affected by the rainfall duration, rainfall intensity, initial groundwater conditions, and hydraulic properties of soil, which in turn affects the settlement response heavily. The bearing capacity is evaluated using graphical methods via the load–settlement response curves, and it was found that the reduction in matric suction heavily reduces the bearing capacity of the soil. Combined with the unsaturated residual soils and transient analyses, the discoveries give insight into the assessment of shallow foundations subjected to water infiltration.

Keywords: shallow foundation; bearing capacity; settlement; infiltration; numerical analysis

1. Introduction

Over the years, climate change has not only affected Singapore, but has made a global impact. Singapore, as a country, has many plans to tackle climate change and the effects that stem from it. Site-based studies in the city—East Coastal Region of Singapore are carried out and a Coastal and Flood Protection Fund has been set up by the government, with an initial fund injection of SGD 5 billion; these are some of the few strategies used to tackle the risk of coastal flooding due to rising sea levels [1,2]. Other than rising sea levels, the climate change effect has also been shown to increase the number of rain days and extreme rainfall events [3–5].

Singapore has already been experiencing inter-monsoon periods in the month of October and November [6]. More recently, floods in many areas of Singapore [7], more notably, floods in the Bukit Timah vicinity, have been caused by these monsoon seasons. The Bukit Timah area has many land properties built on shallow foundations that are susceptible to floods and heavy rainfall. Water ingress into motor vehicles and low-rise properties, both residential and commercial, were unavoidable during the flood, resulting in damages and traffic delays in the Bukit Timah and Dunearn Road precincts [8] Toll et al. [9] pointed out that many low-rise constructions suffer from potential collapse and heavy

settlements caused by groundwater level rise, either from floods or heavy rain. This is attributed to the 10% increase in moisture content of clay which increases settlement by 2–3 times [10] and the increase in the degree of saturation that comes with the groundwater table rise [11]. Singapore is a tropical country that experiences monsoon seasons per year with constant heavy rainfall all year round. Singapore is also geographically hilly, with plenty of gentle and steep slopes around the island. Thus, there are numerous studies involving rainfall-induced slope failure. Despite many studies of rainfall events on soil slopes and the impacts on slope stability in Singapore, there are little studies carried out on the response of shallow foundations under rainfall events in Singapore [4,5,12–15]. Globally, laboratory and field studies have been carried out on the impact of rising groundwater level on foundation settlements; these studies generally found that an increase in groundwater level and soil moisture increased soil's deformations and settlements by up to 100% [16].

Jeong et al. [17] and Kim et al. [18] simulated field load tests of shallow foundations using finite element methods (FEM) and found reasonable agreement when comparing simulated and field test results. They also concluded that shallow foundations of higher dimensions experience a higher settlement as compared to those of lower dimensions. This size effect can be accounted for by plotting applied loading against normalized settlement curves [19]. Thus, in this study, different sizes of shallow foundations were not considered as a controlling parameter for the load–settlement response. In the same study, the matric suction measured in the field after rainfall was compared against simulated rainfall using a FEM, and was found to be reasonably agreeable. This simulated matric suction was imported to an independent sequential analysis, where the rainfall was simulated first, and the resulting matric suction was used to perform a load-deformation analysis. However, the nature of rainfall is such that it is a transient and time-dependent process. Thus, in this study, a coupled flow-deformation analysis was used to simulate both rainfall and shallow foundation response simultaneously [20], with the aim of simulating the deformation response due to changes in hydraulic conditions and transient pore-water pressure of residual soil in the area of Bukit Timah Granit.

Conventional design for shallow foundations has always assumed that the soil is fully saturated. However, shallow foundations typically sit on unsaturated soils with the groundwater table far below surface level. This leads to an overestimation of settlement, and discrepancies between actual and estimated settlement. This problem is exacerbated when rainfall is introduced and seeps into the soil, causing a change in matric suction of the soil. This change in matric suction will alter many soil properties, e.g., elastic modulus and shear strength to the hydraulic conductivity of the soil.

This study attempts to evaluate the impact of climate change-induced heavy rainfall events on the stability of shallow foundations in the Bukit Timah region in Singapore using finite element methods (FEM). The results obtained from this study will serve as a reference for engineers to provide sufficient considerations for unsaturated soil transient rainfall infiltration conditions, specifically, for shallow foundation purposes. Two-dimensional (2D) coupled flow-deformation analyses were carried out using commercial software, SIGMA/W [21]. Bukit Timah Granite (BTG) residual soil was used as the main soil type in this analysis. Boundary conditions of rainfall intensity, duration, and the groundwater table position varied through parametric studies to explore the influence of these controlling parameters on the load–settlement response of the shallow foundation in BTG.

2. Methodology

2.1. Geographical and Geological Setting

Residual soils in Singapore are characterized by a parent rock formation that mainly comprises at least three formations, such as Jurong Formation, Bukit Timah Granite, and Old Alluvium [22]. Figure 1 illustrates a simplified Singapore geological map outlining the distribution of geological formations. In particular, the Bukit Timah Granite historically dominates Singapore's geological formation, which comprises five discrete and contiguous plutons [23]. As discovered mainly from visual observation, the residual soil is the final

product of the in-situ weathering of underlying rocks and its shear strength is dependent on the degree of weathering [24]. Numerous researchers in Singapore [22,25–27] explored variabilities of residual soil properties in terms of mechanical and hydraulic characteristics along with depths. Rahardjo et al. [25] stated that the typical effective cohesion of residual soils in Bukit Timah Granit decreases with depth due to the reduction in fine fractions and ranges from 8 kPa to 24 kPa over Singapore. Kim et al. [22] pointed out that the variability of effective cohesion in Bukit Timah Granit can be clearly differentiated with the incorporation of artificial intelligence techniques, ranging from 4 kPa to 16.5 kPa. Ip et al. [26] observed the variability of hydraulic properties of the residual soil in Bukit Timah Granit, having a wide range of air-entry values due to the large variety of particle sizes. In addition, Satyanaga et al. [27] proposed upper and lower limits for residual soil's mechanical and hydraulic properties in Bukit Timah Granit.
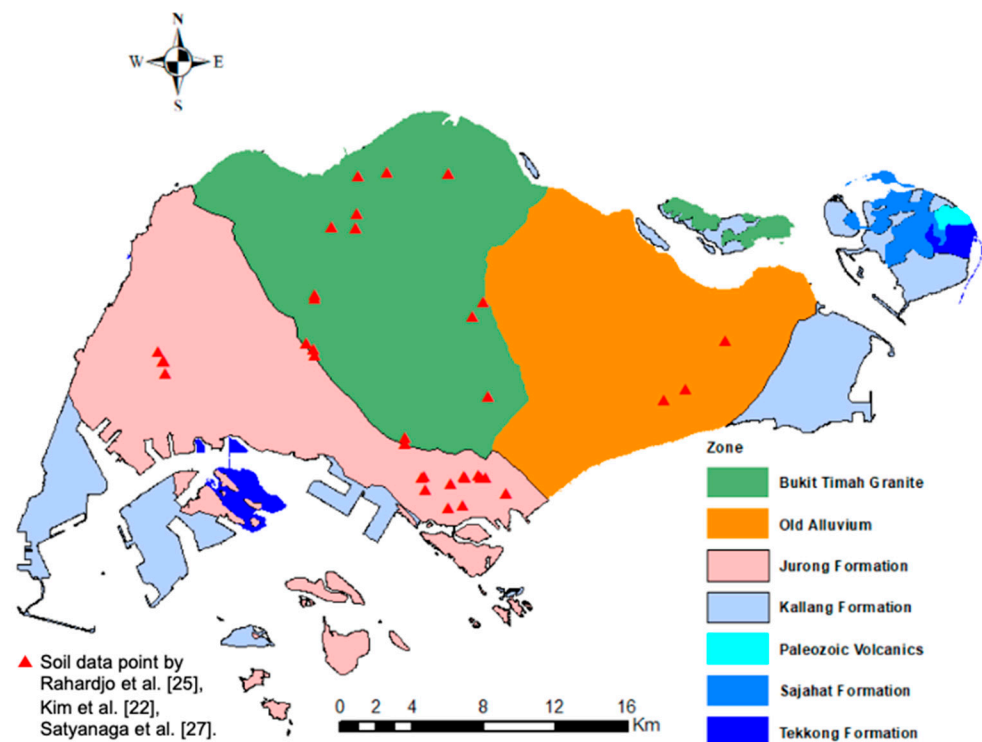

Figure 1. Distribution of Singapore geological formations and soil database points studied by researchers [22,25,27]. (modified from Kim et al. [22]).

This study focuses on the area of Bukit Timah Granit to explore the settlement behavior of shallow foundations situated in residual soil in Bukit Timah Granit.

2.2. Evaluation of Bearing Capacity from Load–Settlement Responses

Load-settlement data from loading tests can be used to evaluate the bearing capacity of the soil through graphical methods. In this study, two methods, the Brinch Hansen method by Hansen [28] and the Chin–Kondner Extrapolation method by Chin [29], were used to extrapolate the ultimate bearing capacity of the soil. Data obtained from the FEM analysis were used to perform these estimations. The estimation methods were not meant to accurately predict the ultimate bearing capacity of the foundations in this study, but to observe the trends in ultimate bearing capacity in relation to the changes in matric suction, duration of rainfall and the rainfall intensity.

2.2.1. Brinch Hansen 80% Criterion

Hansen [28], when discussing Kondner's [30] work, proposed an approximation of the hyperbolic stress–strain behavior of cohesive soils during triaxial testing, and observed

that a general failure criterion can be inferred from the equations: the failure stress is determined by the strain that is four times the strain of stress and is 20% less than the failure stress. Thus, this method is known as the Brinch Hansen 80% failure criterion. This method can be applied graphically to determine the ultimate bearing capacity by squaring rooting the settlement of each data point and then dividing it by the load value. This value is plotted against the settlement in a graphical method that gives a linear relationship after a certain point. The linear relationship gives rise to a trend line with a slope and y-intercept, and is used to determine the ultimate bearing capacity (Q_u) below:

$$Q_u = \frac{1}{2\sqrt{C_1 \times C_2}} \tag{1}$$

where C_1 is the slope of the linear trend line, and C_2 is the y-intercept of the linear trend line.

2.2.2. Chin–Kondner Extrapolation Method

This method by Chin [29] stems from Kondner's [30] work, which extrapolates the ultimate loads of a load test, without loading the components to fail. The method divides the settlement by the load and plots the values against the settlement. The corresponding graph also shows a linear relationship after a certain point. The inverse of the slope of this linear trend line gives the ultimate bearing capacity.

$$\frac{\Delta}{P} = C_1 \Delta + C \tag{2}$$

where Δ is settlements, P is the load, C_1 is the slope, and C is the constant.

$$Q_u = \frac{1}{C_1} \tag{3}$$

2.3. Estimation of Unsaturated Elastic Modulus

Soil properties are affected by the degree of saturation and matric suction of the soil. Rainfall infiltration into dry soil increases the degree of saturation and reduces the matric suction, along with the increased shear strength and stiffness that stems from the high matric suction. As such, in a study of rainfall infiltration into soils, it is important to estimate and compare the stiffness of the soils before, during and after rainfall

A semi-empirical model by Vanapalli and Oh [31] is able to predict the modulus of elasticity with respect to the matric suction of the soil.

$$E_{i(unsat)} = E_{i(sat)} \left[1 + \alpha \frac{u_a - u_w}{p_a / 101.3} S^\beta \right] \tag{4}$$

The model was developed using the SWCC and the saturated elastic modulus of the soil, along with fitting parameters α and β. The terms $E_{i(unsat)}$ and $E_{i(sat)}$ are the initial unsaturated and saturated tangent elastic modulus, respectively. p_a is the atmospheric pressure (101.3 kPa), while S is the degree of saturation. In the equation, the parameters α and S^β control the non-linear variation of the unsaturated elastic modulus. When the soil reaches residual saturation conditions, the degree of saturation approaches, while the matric suction ($u_a - u_w$) increases to larger numbers. In this study, the $E_{i(unsat)}$ is found using the α factor of 0.1, and the β factor of 2.0. The α factor is a function of the plasticity index of the soil, and the β can be either 1.0 for coarse-grained soils, or 2.0 for fine-grained soils. The matric suction and degree of saturation were obtained from the FEM model for consistency with the simulated results. The SIGMA/W software was unable to implement this model to simulate the changes in stiffness with regard to the change in matric suction under rainfall infiltration. However, a comparison was made in a further section of the study, where the simulated SIGMA/W results were compared against a calculated empirical settlement, using this model as a determinant for soil stiffness.

2.4. Finite Element Modelling and Input Parameters

The 2D plane-strain finite element model for the analysis of rainfall infiltration into Bukit Timah Granite (BTG) soil was developed. The SIGMA/W was used to create the shallow foundation model with a 10 B in width and 5 B in height, where B (=5 m) is the width of the footing in the FEM. The mesh of the model was discretized into a global size of 0.75 m, with secondary nodes enabled for 8-noded element mesh for strain-stress analysis. The left and right side of the model was fixed in the horizontal direction, while the bottom of the soil model was fixed in both a horizontal and vertical direction. A no-flow boundary condition was also applied to the sides and bottom of the model, and less water flowed out of the model in those directions. Floods and run-off resulting from the rainfall and the lack of infiltration capacity of the soil were also disregarded in this study. Figure 2 shows the FE mesh and boundary conditions. Loads were applied to simulate a load of a building in increments of 100 kPa, starting from 100 kPa and ending at 500 kPa, and were applied at the surface of the soil in the center of the model to investigate the load–settlement response.
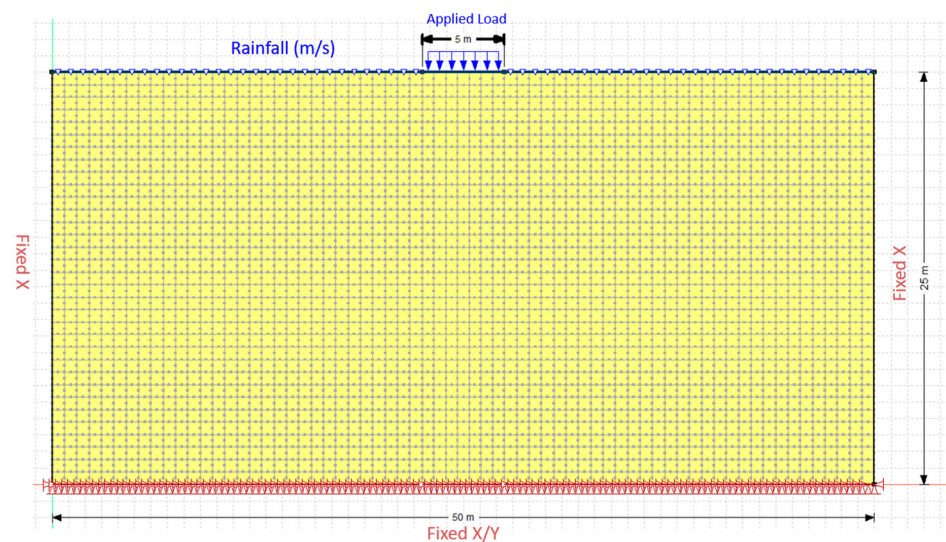

Figure 2. The 2D finite element (FE) model used in this study.

The soil parameters of residual soil in BTG were adapted from Rahardjo et al. [14,25], which were obtained from a study area in Orchard Boulevard situated in the southern part of Singapore. The residual soil was modelled in SIGMA/W using the Mohr-Coulomb model. The soil parameters, along with the hydraulic parameters are presented in Table 1 [14,25]. The soil–water characteristic curve (SWCC) and the unsaturated permeability function were both fitted using the Fredlund and Xing [32] function and were both implemented natively in the SIGMA/W hydraulic modules in GeoStudio. The SWCC and unsaturated permeability functions are presented in Figures 3 and 4.

Table 1. Soil and hydraulic parameters for BTG residual soil [14,25].

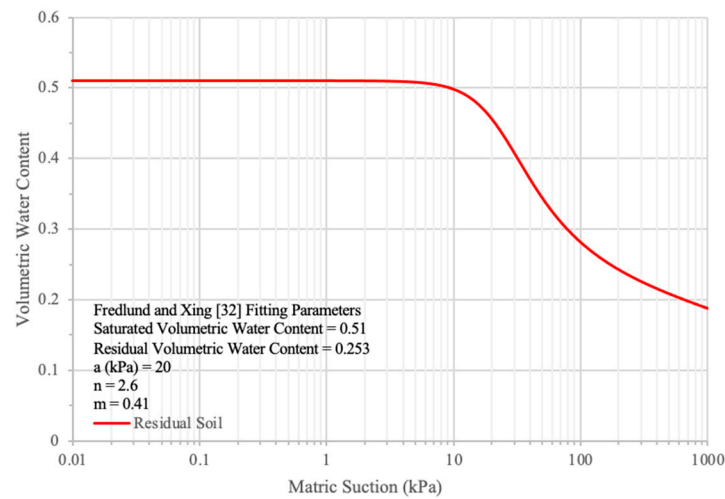| Properties	Residual Soil
Unit Weight, γ (kN/m^3)	18
Saturated Volumetric Water Content, θ_s	0.51
Residual Volumetric Water Content, θ_r	0.253
Saturated Permeability, k_s (m/s)	1.00×10^{-6}
Fredlund and Xing (1994) SWCC Fitting Parameters	
a (kPa)	20
n	2.6
m	0.41
Effective Cohesion, c' (kPa)	5
Effective Friction Angle, ϕ' ($\circ$)	28
Effective Elastic Modulus, E (mPa)	20
Initial Void Ratio, e_0	0.8

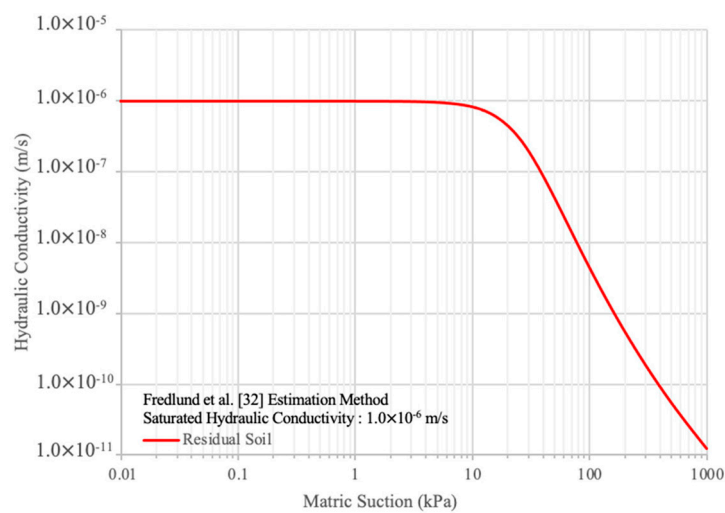**Figure 3.** Soil–water characteristic curve for BTG residual soil.

Figure 4. Unsaturated permeability function for BTG residual soil.

Rainfall events of 8 mm/h, 20 mm/h and 32 mm/h were applied for 1, 2, 3, 4 and 5 days to the ground surface [4]. A rainfall event of 0 mm/h rainfall for similar durations was also modeled to study the 0 rainfall condition and understand the scenario of a lack of rainfall. The rainfall intensities and durations were adapted from Kim et al. [4], which were

determined based on historical maximum daily rainfalls and obtained from meteorological stations in Singapore. The adapted values had a slight increase in intensity to factor in the impacts of climate change. Initial groundwater tables of 1 B m and 2 B m below the surface were adopted, which gave an initial matric suction of 50 kPa and 100 kPa, respectively. These controlling parameters used in the simulations are summarized in Table 2. The coupled flow-deformation analyses were performed to simulate the time-dependent transient water flow/infiltration and the deformation response in response to flux boundary conditions [4]. No ponding boundary condition at the surficial layer was considered. The sequential analysis procedure used in this study is summarized in Figure 5.

Table 2. Summary of controlling parameters used in the simulations.

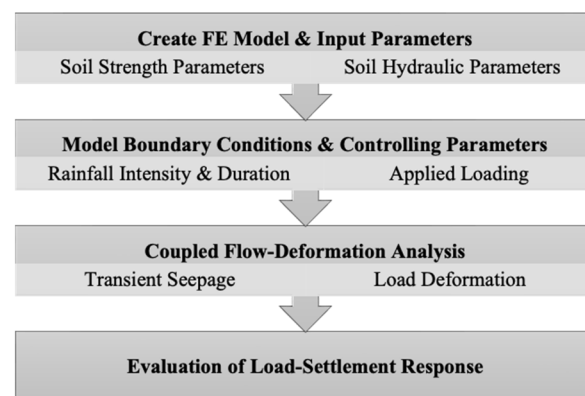| Soil Type	Footing Size	Groundwater Table Position	Rainfall Intensities	Duration
Bukit Timah Granite Residual Soil	5 m width	5 m/10 m below ground level	0 mm/h 8 mm/h 20 mm/h 32 mm/h	1 day 2 day 3 day 4 day 5 day

**Figure 5.** Sequential processes of finite element (FE) analysis.

3. Simulation Results

3.1. Effects of Rainfall Intensity and Duration on Matric Suction Changes

Changes in the matric suction of the model were plotted against the rainfall intensities in various groundwater table locations in Figure 6. A general trend was observed between the two different groundwater table locations, where the initial matric suction decreased greatly at the 8 mm/h rainfall intensity but reached a constant after the 20 mm/h rainfall intensity. This could be attributed to the infiltration capacity of the soil, where it reached its maximum capacity at 20 mm/h of rainfall. Thus, the rate of the decreasing matric suction remained constant. A difference in initial matric suction of the two different groundwater table locations also affected the initial infiltration capacity of the soil, where it was lower as compared to fully saturated soil due to the increase in tensile forces between the soil particles and water, restricting the incoming rainfall infiltration's flow path, thus, decreasing the permeability [33].
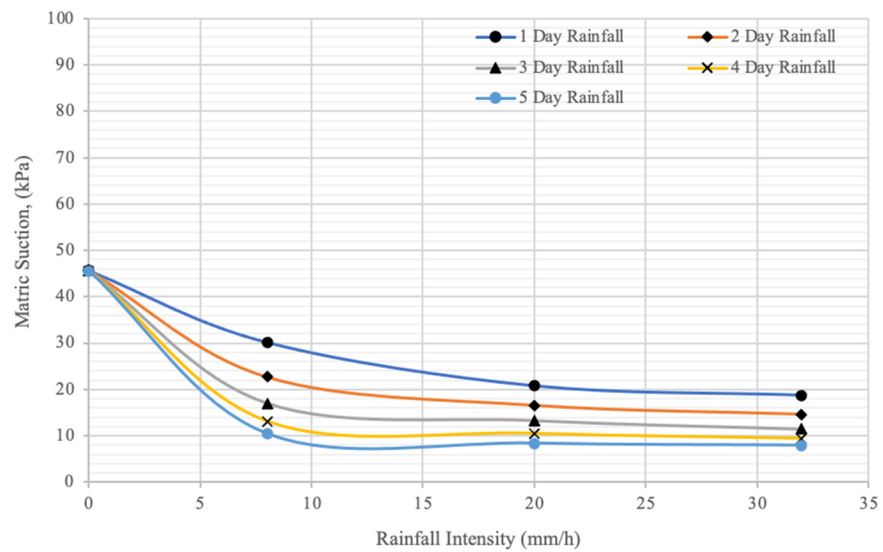
(**a**) Groundwater table 5 m below
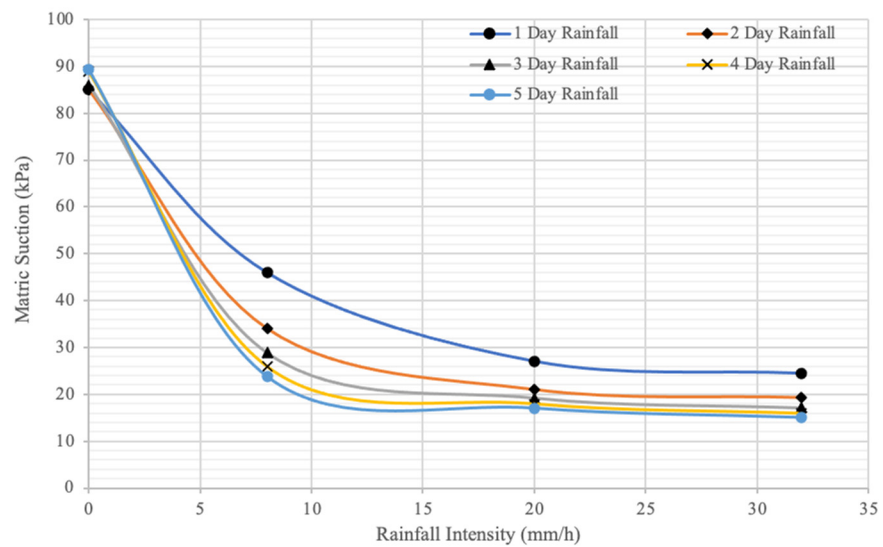
(**b**) Groundwater table 10 m below

Figure 6. Effects of rainfall intensity on the matric suction (500 kPa applied loading).

Another trend observed in the curves was the difference in matric suctions between the different durations of rainfall. Despite reaching a steady state of matric suction after 20 mm/h of rainfall intensity and the maximum infiltration capacity, increases in the duration of rainfall also decreased the matric suction by a particular amount. Due to the maximum capacity of infiltration reached, only with a longer time period can the water infiltrate through the soil and decrease the matric suction, along with increasing the groundwater table. This is usually the case for soils with lower permeability, where rainfall with higher durations and a lower intensity is applied to the soil to study the change in matric suction, while the reverse is true for soils with higher permeability [4,12–14].

3.2. Effects of Initial Matric Suction on the Load Settlement Response

The load–settlement curve of both groundwater tables under 1 day of rainfall duration is presented in Figure 7. The load–settlement response between the groundwater table at 5 m and 10 m differed significantly, with or without rainfall. Without rainfall, the initial matric suction difference gave the soil a higher bearing capacity; thus, at the groundwater

Table 10 m below, the load–settlement response was less steep as compared to the groundwater Table 5 m below. It is also observed that the load–settlement response did not differ significantly between the 0 rainfall and the 8 mm/h rainfall intensity. The higher initial matric suction reduced the initial permeability greatly, and the 8 mm/h rainfall intensity did not saturate the soil significantly enough to lower the bearing capacity of the soil when compared to the 0 rainfall scenario. The observed curves of 20 mm/h and 32 mm/h rainfall were also steeper in the 10 m groundwater table due to the higher change in the matric suction, from the initial matric suction to the end of the 1 day of rainfall (Figure 6b). These observations suggest that the initial matric suction plays a big role in the load–settlement response as a result of the change in the matric suction in the soil during and at the end of the rainfall event, as the rainwater infiltrates through the soil and causes the change in the matric suction, which in turn, changes the shear strength and soil stiffness.
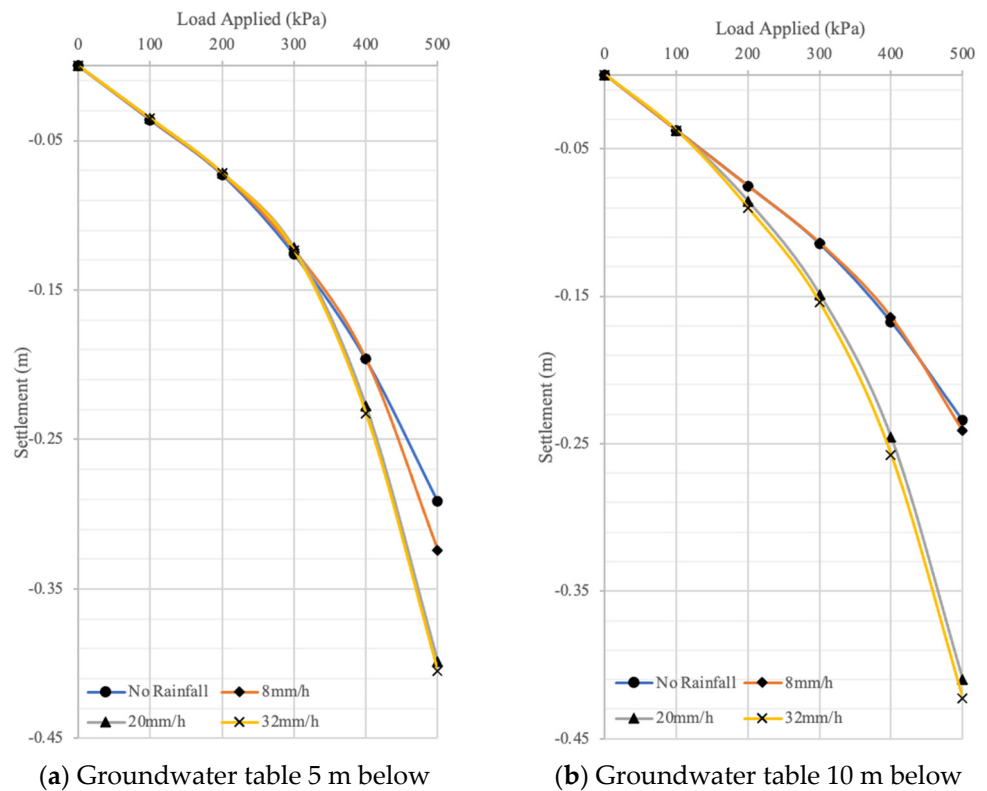

(**a**) Groundwater table 5 m below   (**b**) Groundwater table 10 m below

Figure 7. Load–settlement curves under 1 day of rainfall.

3.3. Effects of Rainfall Intensity and Duration on Load Settlement Response

The load–settlement response curves are plotted and presented in Figures 8 and 9 with respect to the rainfall intensity of 8 mm/h and 20 mm/h, and the groundwater table at 5 m and 10 m below ground level [4]. Generally, it is observed that the settlement response was greater under higher rainfall intensities and under the rainfall infiltration condition, which was limited to the soil's infiltration capacity. Effectively, the change in the settlement between rainfall duration and rainfall intensity can be linked to the change in the matric suction of the soil undergoing rainfall infiltration.
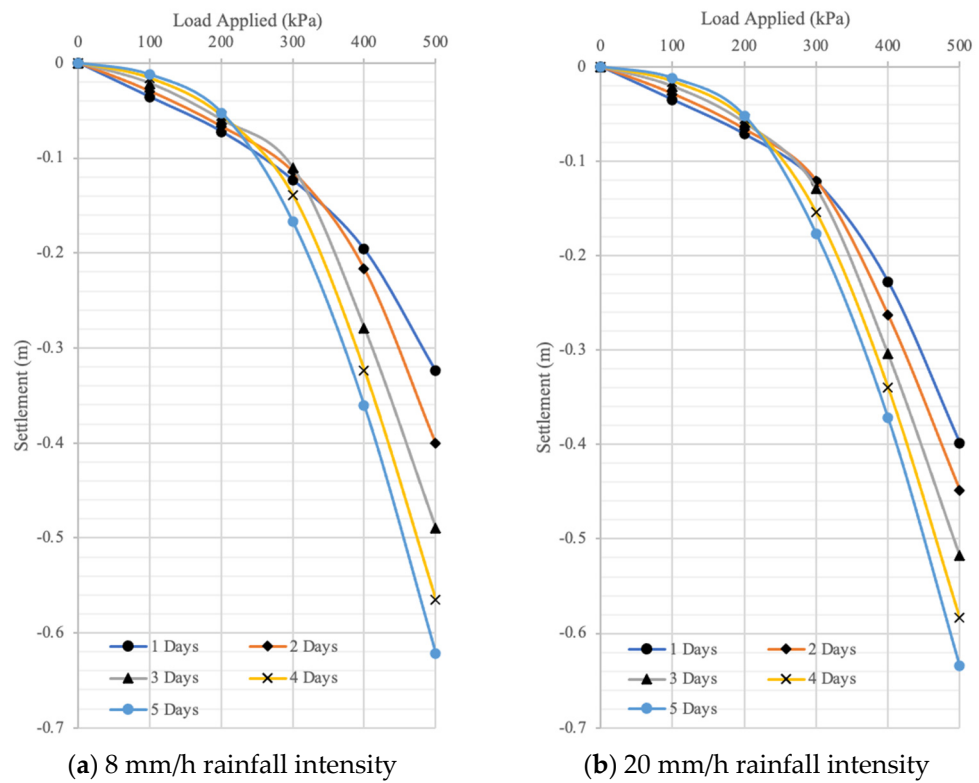
(**a**) 8 mm/h rainfall intensity   (**b**) 20 mm/h rainfall intensity

Figure 8. Load–settlement curves (groundwater table 5 m below).

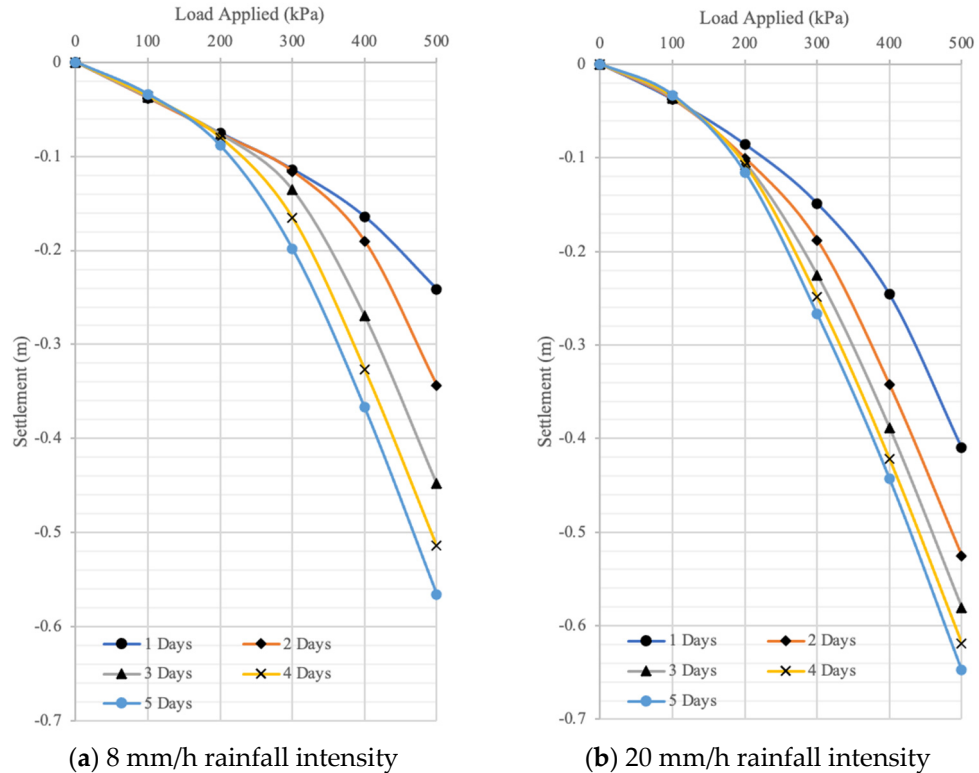(**a**) 8 mm/h rainfall intensity   (**b**) 20 mm/h rainfall intensity

Figure 9. Load–settlement curves (groundwater table 10 m below).

3.4. Comparison of FE Results and Empirical Calculations

The settlement of the model under 500 kPa of applied loading was compared against a calculated settlement with the same parameters. The graphs in Figure 10 are plotted as a

duration–settlement curve; the percentage difference in settlement was found in the FEM and the empirical calculation against the settlement was observed when the soil was fully saturated. The settlement at full soil saturation was found using SIGMA/W through a load/deformation analysis with an applied loading of 500 kPa, with the groundwater table at ground level. The calculated settlement utilized a calculated unsaturated elastic modulus found in Equation (4) through a semi-empirical model by Vanapalli and Oh [31], where the model is able to predict the modulus of elasticity with respect to the matric suction of the soil.
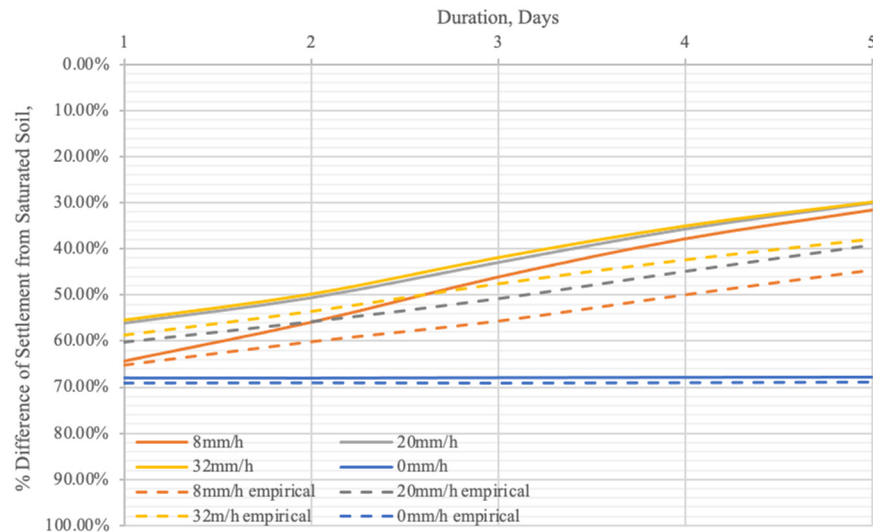
(**a**) Groundwater table 5 m below
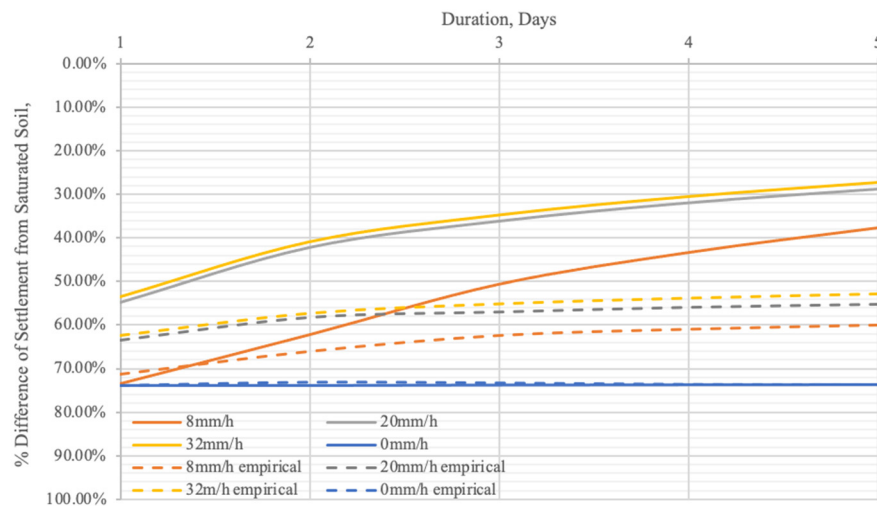
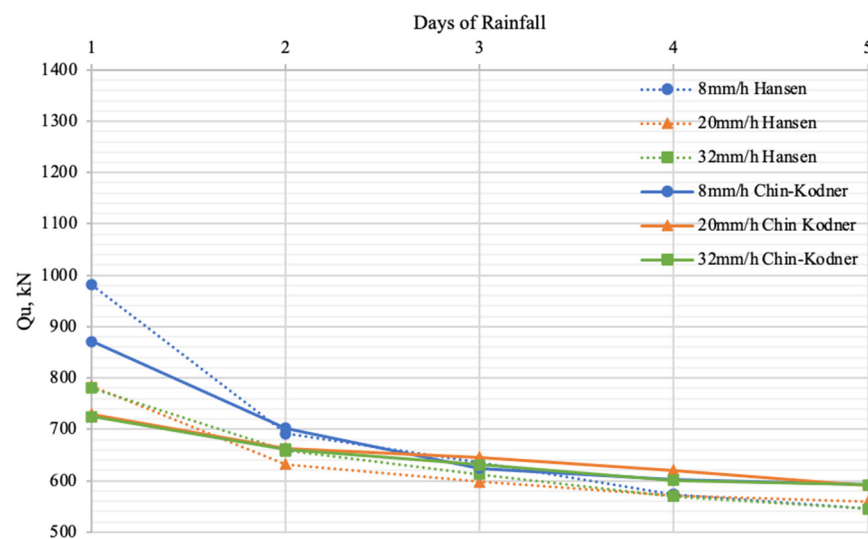(**b**) Groundwater table 10 m below

Figure 10. Comparison of time–settlement curves between FE and calculated results.

The predicted unsaturated elastic modulus was used to calculate the settlement of the shallow foundation through the elastic settlement equation by Timošenko and Goodier [34]. The results of the comparison can be observed in Figure 10. The trend observes the empirically calculated results underestimated the settlement when compared to the FEM-simulated results. The under-prediction ranged from 4% to 12% for a groundwater table of 5 m below ground level, which is reasonable when comparing empirical calculations against simulated results. Meanwhile, the under-prediction of the calculation of the groundwater table of 10 m below ground level was much higher, in the 22% to 26% range.

The under-prediction of settlement by the semi-empirical model can be attributed to the over-prediction of the unsaturated elastic modulus. According to Vanapalli and Oh [31], their model was found to be overpredicting the unsaturated elastic modulus for the matric suction range of 0–100 kPa. This over-prediction results in an underestimation of the settlement, which explains the under-prediction of the settlement when compared to the simulated FEM. It should be noted that the semi-empirical model by Vanapalli and Oh [31] has not been validated for the wetting path of the SWCC.
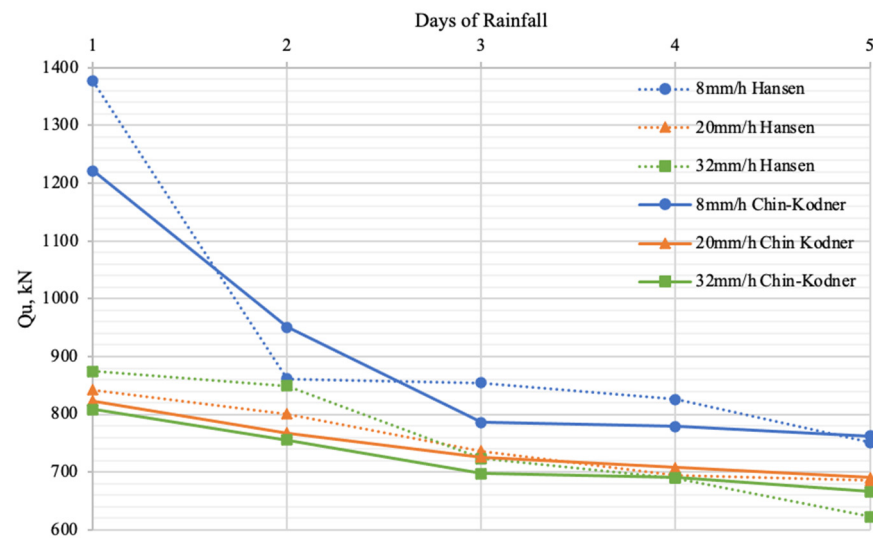
3.5. Estimation of Soil Bearing Capacity from Load–Settlement Response Curves

An estimated ultimate bearing capacity of the soil can be evaluated using different methods through the analysis of the load–settlement curves. In this study, the Hansen 80% Criterion by Hansen [28] and the Chin–Kondner extrapolation method by Chin [29] was used to plot the graphs in Figure 11, where the resultant ultimate load was plotted against the number of rainfall days. In both figures, the bearing capacity can be observed to be high, while dropping with the increase in days of rainfall. This was much more prominent in the 8 mm/h rainfall curve, where the initial bearing capacity at 1 day of rainfall was very high due to the high matric suction and a low degree of saturation of the soil, falling drastically at 3–5 days of rainfall. At the 5-day rainfall, the curves are narrowly spaced together, due to the soil nearing full saturation, resulting in roughly the same matric suction, and thus, the same shear strength.

(**a**) Groundwater table 5 m below

Figure 11. *Cont.*

(**b**) Groundwater table 10 m below

Figure 11. Estimation of soil bearing capacity.

4. Discussion

The impact of the rainfall in the BTG soil depends on the rainfall duration, rainfall intensity and initial groundwater conditions. The results obtained from this study were severely limited by the BTG residual soil's hydraulic characteristics and were observed through the numerous similar data points in the 20 mm/h and 32 mm/h rainfall intensity scenarios. A larger difference was observed between the 8 mm/h and 20 mm/h scenarios, where the changes in matric suction are more apparent, and the different trends in the impact of the rainfall intensities can be observed. It is apparent that in a short-duration rainfall scenario (one to two days), the variations in rainfall intensities do not affect the settlements to a large extent.

High rainfall intensities with short rainfall durations are only important when the groundwater table is low (10 m below ground level). However, despite the high groundwater table in Singapore, floods do occur on a frequent basis during monsoon seasons [4]. It is known that the matric suction greatly affects the hydraulic properties of the soil [35]. In the case of climate change causing extreme weather phenomena, the lowering of the groundwater table due to long periods of non-rainfall [5], coupled with a climate change-amplified downpour, may lead to intense floods in Singapore, along with an increase in settlement for buildings with shallow foundations [36].

Various environments to generate rigorous rainfall scenarios are needed. Through rainfall infiltration and runoff, water transfer across the atmosphere–soil domain occurs due to evaporation or evapotranspiration, which is affected by rainfall, evaporation, initial water contents, air and soil temperatures, and oxygen concentration [35]. These parameters can be measured in fields under asphalt pavement, aeration salb and turf cover in an open space and can significantly affect the amount of rainwater as a flux boundary condition. In order to consider rainfall–runoff–evaporation, reliable hydrological models such as a Sacramento soil moisture accounting model [37] can be utilized to capture and calibrate the actual flux boundary condition. Therefore, measurements and analyses of weather conditions could be incorporated in future studies of foundation stability under transient conditions.

5. Conclusions

The impact of heavy rainfall on shallow foundations in Bukit Timah Granite was investigated numerically using Geo-Slope [21]. The effects of the infiltration of the rainfall into the soil were incorporated into the numerical model through the SWCC and permeability functions, and many different boundary conditions from applied loading, rainfall intensity

and rainfall duration were simulated using the software via fully coupled load-deformation analysis with time-dependent transient rainfall infiltration effects. Comparisons made between simulated FEM results and empirical calculations showed reasonable agreement.

The results have evidently shown that settlement is greatly affected by rainfall events with a high intensity but low duration, or rainfall events with a low intensity but high duration, or a combination of both high intensity and high duration of rainfall. With climate change causing extreme weather patterns, such rainfall events are unavoidable.

Further studies based on the limitations of this study can be recommended. By implementing the complete geological profile of the Bukit Timah Granite Formation, a more comprehensive study can be performed on the impact of climate change-induced rainfall events on the Bukit Timah Granite soils. Alternatively, a study on compacted residual soil of the Bukit Timah Granite variety can be performed and the impact can be evaluated and compared in terms of the change in the settlement, bearing capacity and even the hydraulic capacity with regard to flooding and rainfall infiltration. In addition, reliable hydrological models such as soil moisture accounting (SMA) can be incorporated into the simulation for rigorous analyses.

References

1. National Climate Change Secretariat. Coastal Protection. National Climate Change Secretariat. 2021. Available online: https://www.nccs.gov.sg/singapores-climate-action/coastal-protection/ (accessed on 1 September 2021).
2. Parliment of Singapore. *Measures in Place to Manage Rising Sea Levels and Unpredictable Weather Patterns*; Parliment of Singapore: Singapore, 2022.
3. Guhathakurta, P.; Sreejith, O.P.; Menon, P.A. Impact of climate change on extreme rainfall events and flood risk in India. *J. Earth Syst. Sci.* **2011**, *120*, 359–373. [CrossRef]
4. Kim, Y.; Rahardjo, H.; Nistor, M.M.; Satyanaga, A.; Leong, E.C.; Sham, A.W.L. Assessment of critical rainfall scenarios for slope stability analyses based on historical rainfall records in Singapore. *Environ. Earth Sci.* **2022**, *81*, 39. [CrossRef]
5. Satyanaga, A.; Kim, Y.; Hamdany, A.H.; Nistor, M.M.; Sham, A.W.L.; Rahardjo, H. Preventive measures for rainfall-induced slope failures in Singapore. In *Climate and Land Use Impacts on Natural and Artificial Systems*; Elsevier: Amsterdam, The Netherlands, 2021; pp. 205–223.
6. Meteorological Service Singapore. *More Thundery Showers Expected in First Half of November 2021*; Meteorological Service Singapore: Singapore, 2021.
7. Menon, M. Risk of flash floods in several areas, including Pasir Panjang, Dunearn Road. *The Straits Times*, 18 November 2021.
8. Lim, V. After Recent Floods, Bukit Timah Residents and Businesses Take Precautions to Stay Dry. *Channel News Asia*, 8 September 2021.
9. Toll, D.G.; Abedin, Z.; Buma, J.; Cui, Y.; Osman, A.S.; Phoon, K.K. *The Impact of Changes in the Water Table and Soil Moisture on Structural Stability of Buildings and Foundation Systems: Systematic Review CEE10-005 (SR90)*; Technical Report; Collaboration for Environmental Evidence, 2012.
10. Čajk, R.; Manasek, P. Building structures in danger of flooding. In Proceedings of the Role of Structural Engineers towards Reduction of Poverty: IABSE Conference, New Delhi, India, 19–22 February 2005; pp. 551–558.
11. El-Ehwany, M.; Houston, S.L. Settlement and Moisture Movement in Collapsible Soils. *J. Geotech. Eng.* **1990**, *116*, 1521–1535. [CrossRef]
12. Kristo, C.; Rahardjo, H.; Satyanaga, A. Effect of variations in rainfall intensity on slope stability in Singapore. *Int. Soil Water Conserv. Res.* **2017**, *5*, 258–264. [CrossRef]
13. Rahardjo, H.; Nio, A.S.; Leong, E.C.; Song, N.Y. Effects of Groundwater Table Position and Soil Properties on Stability of Slope during Rainfall. *J. Geotech. Geoenviron. Eng.* **2010**, *136*, 1555–1564. [CrossRef]

14.   Rahardjo, H.; Kim, Y.; Gofar, N.; Leong, E.C.; Wang, C.L.; Wong, J.L.H. Field instrumentations and monitoring of GeoBarrier System for steep slope protection. *Transp. Geotech.* **2018**, *16*, 29–42. [CrossRef]

15.   Rahardjo, H.; Kim, Y.; Satyanaga, A. Role of unsaturated soil mechanics in geotechnical engineering. *Int. J. Geo-Eng.* **2019**, *10*, 8. [CrossRef]

16.   Shahriar, M.; Sivakugan, N.; Das, B. Settlements of Shallow Foundations in Granular Soils Due to Rise of Water Table—A Critical Review. *Int. J. Geotech. Eng.* **2012**, *6*, 515–524. [CrossRef]

17.   Jeong, S.; Kim, Y.; Park, H.; Kim, J. Effects of Rainfall Infiltration and Hysteresis on the Settlement of Shallow Foundations in Unsaturated Soil. *Environ. Earth Sci.* **2018**, *77*, 494. [CrossRef]

18.   Kim, Y.; Park, H.; Jeong, S. Settlement Behavior of Shallow Foundations in Unsaturated Soils under Rainfall. *Sustainability* **2017**, *9*, 1417. [CrossRef]

19.   Briaud, J.-L. Spread Footings in Sand: Load Settlement Curve Approach. *J. Geotech. Geoenviron. Eng.* **2007**, *133*, 905–920. [CrossRef]

20.   Rahardjo, H.; Kim, Y.; Gofar, N.; Satyanaga, A. Analyses and design of steep slope with GeoBarrier system (GBS) under heavy rainfall. *Geotext. Geomembr.* **2020**, *48*, 157–169. [CrossRef]

21.   *GEOSTUDIO User's Manual*; Geo-Slope International Ltd.: Calgary, AB, Canada, 2021.

22.   Kim, Y.; Satyanaga, A.; Rahardjo, H.; Park, H. Estimation of effective cohesion using artificial neural networks based on index soil properties: A Singapore case. *Eng. Geol.* **2021**, *289*, 106163. [CrossRef]

23.   Singapore Geology. *Building and Construction Authority (BCA)*; Singapore Geology: Singapore, 2021.

24.   Little, A.L. The engineering classification of residual tropical soils. In Proceedings of the 7th International Conference Soil Mechanics and Foundation Engineering, Mexico City, Mexico, 25–29 August 1969; Volume 1, pp. 1–10.

25.   Rahardjo, H.; Satyanaga, A.; Leong, E.C.; Ng, Y.S.; Pang, H.T.C. Variability of residual soil properties. *Eng. Geol.* **2012**, *141–142*, 124–140. [CrossRef]

26.   Ip, C.Y.; Rahardjo, H.; Satyanaga, A. Spatial Variations of Air-entry Value for Residual Soils in Singapore. *Catena* **2019**, *174*, 259–268. [CrossRef]

27.   Satyanaga, A.; Rangarajan, S.; Rahardjo, H.; Li, Y.; Kim, Y. Soil database for development of soil properties envelope. *Eng. Geol.* **2022**, *304*, 106698. [CrossRef]

28.   Hansen, J.B. Discussion of Hyperbolic Stress-Strain Response: Cohesive Soils. by Robert L. Kondner. *J. Soil Mech. Found. Div.* **1963**, *89*, 241–242. [CrossRef]

29.   Chin, F.K. Estimation of the ultimate load of piles from tests not carried to failure. In Proceedings of the 2nd Southeast Asian Conference on Soil Engineering, Singapore, 11–15 June 1970.

30.   Kondner, R.L. Hyperbolic Stress-Strain Response: Cohesive Soils. *J. Soil Mech. Found. Div.* **1963**, *89*, 115–143. [CrossRef]

31.   Vanapalli, S.; Oh, W. A model for predicting the modulus of elasticity of unsaturated soils using the soil-water characteristic curve. *Int. J. Geotech. Eng.* **2010**, *4*, 425–433. [CrossRef]

32.   Fredlund, D.G.; Xing, A. Equations for the Soil-Water Characteristic Curve. *Can. Geotech. J.* **1994**, *31*, 521–532. [CrossRef]

33.   van Genuchten, M.; Pachepsky, Y.A. Hydraulic Properties of Unsaturated Soils. In *Encyclopedia of Agrophysics*; Gliński, J., Horabik, J., Lipiec, J., Eds.; Springer: Dordrecht, The Netherlands, 2011; pp. 368–376.

34.   Timošenko, S.P.; Goodier, J.N. *Theory of Elasticity*, 3rd ed.; McGraw-Hill: New York, NY, USA, 2004.

35.   Indrawan, I.G.B.; Rahardjo, H.; Leng, E.C.; Tan, P.Y.; Fong, Y.K.; Sim, E.K. Field instrumentation for monitoring of water, heat, and gas transfers through undaturated soils. *Eng. Geol.* **2012**, *151*, 24–36. [CrossRef]

36.   Kim, Y.; Jeong, S. Modeling of shallow landslides in an unsaturated soil slope uing a coupled model. *Geomech. Eng.* **2017**, *13*, 343–370.

37.   Sorooshian, S.; Duan, Q.; Gupta, V.K. Calibration of rainfall-runoff models: Application of global optimization to the Sacramento soil moisture accounting model. *Water Resour. Res.* **1993**, *29*, 1185–1194. [CrossRef]